Shap. Mem. Superelasticity (2016) 2:310–316
DOI 10.1007/s40830-016-0083-y

SPECIAL ISSUE: ADVANCES IN EXPERIMENTATION AT MULTIPLE LENGTH SCALES IN SHAPE MEMORY ALLOYS, INVITED PAPER

On the Transformation Behavior of NiTi Shape-Memory Alloy Produced by SLM

Mathew Speirs[1] · X. Wang[2] · S. Van Baelen[1] · A. Ahadi[3] · S. Dadbakhsh[1] · J.-P. Kruth[1] · J. Van Humbeeck[2]

Published online: 9 November 2016

Abstract Selective laser melting has been applied as a production technique of nickel titanium (NiTi) parts. In this study, the scanning parameters and atmosphere control used during production were varied to assess the effects on the final component transformation criteria. Two production runs were completed: one in a high (~1800 ppm O_2) and one in a low-oxygen (~220 ppm O_2) environment. Further solution treatment was applied to analyze precipitation effects. It was found that the transformation temperature varies greatly even at identical energy densities highlighting the need for further in-depth investigations. In this respect, it was observed that oxidation was the dominating factor, increased with higher laser power adapted to higher scanning velocity. Once the atmospheric oxygen content was lowered from 1800 to about 220 ppm, a much smaller variation of transformation temperatures was obtained. In addition to oxidation, other contributing factors, such as nickel depletion (via evaporation during processing) as well as thermal stresses and textures, are further discussed and/or postulated. These results demonstrated the importance of processing and material conditions such as O_2 content, powder composition, and laser scanning parameters. These parameters should be precisely controlled to reach desired transformation criteria for functional components made by SLM.

✉ Mathew Speirs
mathew.speirs@kuleuven.be

[1] Department of Mechanical Engineering, KU Leuven, Louvain, Belgium

[2] Department of Materials Engineering, KU Leuven, Louvain, Belgium

[3] National Institute for Materials Science, Tsukuba, Japan

Keywords Nickel titanium · Selective laser melting · Shape-memory effect · Transformation temperature · Additive manufacturing

Introduction

Selective laser melting (SLM) is an additive manufacturing (AM) technique allowing fabrication of a wide variety of functional complex three-dimensional parts. Powder layers are melted upon one another locally with a laser beam until part completion [1]. NiTi has been identified as a promising material for SLM aimed at porous biomedical applications [2–4], especially considering its current manufacturing difficulties [5].

Shape-memory alloys (SMAs) such as NiTi have a wide variety of applications in the medical and non-medical fields [6, 7]. This alloy undergoes a reversible phase transformation with temperature from martensite (distorted crystalline monoclinic B19′ lattice with low symmetry) to austenite (ordered crystalline cubic B2 with high symmetry), where the original shape is recovered (thermal memory). In a different scenario when austenite is stable and stressed within a specific temperature, stress-induced martensite (SIM) is formed. This martensite is unstable and as soon as the stress is removed it will revert to austenite upon unloading (superelasticity). These effects occur within a certain temperature range and are highly dependent on the Ni–Ti ratio within a near equiatomic range [8, 9]. Furthermore, it has been reported that the grain size reduction to nanoscale has also significant influence on the internal stress and superelasticity [10].

To produce high-quality functional parts via SLM, all factors affecting the final component transformation criteria must be explored. First, oxygen and carbon [11] pick-up

are known to affect the transformation criteria with powder metallurgy parts containing 1500–3000 ppm oxygen levels [12]. Oxygen and carbon pick-up have been shown to increase linearly in relation to energy density of laser-melted NiTi [13]. Therefore, to keep impurity pick-up to a minimum, this study uses the lowest possible energy density to produce dense (i.e., over 99% density) parts with varied scanning parameters. Second, microstructure has been previously shown to alter depending on SLM process parameters selected for NiTi [14] with high SLM cooling rates affecting the transformation criteria. Third, SLM parts are subject to residual stresses which at identical energy densities are found to be higher for those built at higher scan speeds [15]. Finally, evaporation of nickel due to the nature of SLM can further alter the final transformation temperature [16].

The aim of this work is to further investigate the effect of SLM-processing parameters on the transformation criteria of NiTi bulk parts. The results compliment previously published works [14, 17] by in-depth analyses of SLM process characteristics (such as atmospheric conditions) and their link to transformation temperatures. These provide a clear basis to produce functional NiTi components via SLM.

Materials and Experiments

SLM Process

All parts were produced by an in-house developed SLM machine (Fig. 1) that uses an IPG Yb:YAG fiber laser of 300 W (spot size 80 μm). Plasma-atomized NiTi powder from Raymor Industries Inc., Quebec, Canada, was used. The particle size range was 25–45 μm with a nominal measured Ni content of 55.7 wt% Table 2. An Insta-Trans oxygen sensor from Teledyne analytical instruments (Ontario, Canada) was used for monitoring the O_2 content during processing. These parts were built under argon atmosphere using two different flushings of the argon chamber regimes. One was to produce the lowest possible oxygen content (coded as LO_2, where the chamber was repeatedly flushed until the O_2 content reached about $\sim$220 ppm). The second protocol (coded as HO_2) flushed the chamber twice with argon before processing, allowing $\sim$1800 ppm remaining oxygen. All parts were manufactured with over 99% density using a layer thickness of 30 μm.

Part Design and Production

An overview of all scanning parameters used for SLM in this study is given in Table 1. For this study, cylindrical disks (9 mm in diameter and 3 mm in height) were produced for DSC and XRD. The samples were also solution-treated (ST) at 1000 °C for 120 min after sealing in argon-filled quartz tubes followed by water quenching.

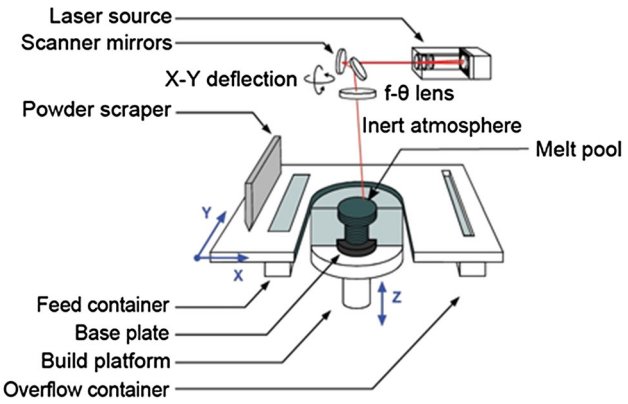

Fig. 1 Schematic illustration of the selective laser melting process (SLM)

Characterization

The transformation behavior was studied by DSC using a TA Q2000 calorimeter with a cooling/heating rate of 10 K min^{-1} in a helium gas atmosphere. To minimize errors of the sample temperature measurements, the samples were attached to a PT-100 sensor, which was used to control the temperature scans. Both as-built and solution-treated samples were assessed from −150 to +150 °C.

The chemical composition analysis was performed using Inductively Coupled Plasma (ICP) method. 100–240 mg of NiTi samples were mixed with 30 mL of HNO_2 and 10 mL of HF in a Teflon beaker and then heated in order to dissolve the samples in the solution. The solution was dried and the residue was dissolved in 40 mL of Aqua regia ($HCl:HNO_3 = 3:1$). The final solution was diluted in a volumetric mask with Mili-Q water, and the concentrations of Ni, Ti, Fe, Cu, Co, and Nb were measured using a Agilent 720-ES ICP instrument.

Further phase identification was completed using a Siemens D500 X-ray diffractometer (XRD) with coupled Theta/2Theta scan type and Cu-Kα1 radiation (wavelength: 0.15418 nm) operated at 40 kV and 40 mA.

Results

Phase Transformation Temperature

The DSC curves of the as-built and solution-treated samples are shown under different oxygen levels in Figs. 2 and 3. The corresponding phase transformation temperatures

Table 1 Overview of scanning parameters used for part production

Laser power (W)	Scanning velocity (mm s^{-1})	Hatch spacing (μm)	Energy density (J mm^{-3})
40	160	75	111
75	313	80	100
100	476	70	100
125	521	80	100
150	714	70	100
175	1167	50	100
200	1333	50	100
225	1250	60	100
250	1042	80	100

are shown in Table 2. As seen in Fig. 2a, the samples produced at high oxygen environment (HO_2) show a clear decrease in transformation temperature with increase of laser power and scanning velocity. Solution treatment of these samples sharpens the peaks, but does not align the peaks for all parameters (Fig. 2b). This may suggest that these parts have undergone some compositional changes according to the used SLM parameters. In contrast, LO_2 samples (Fig. 3) display a much lower range in transformation behavior across the used SLM parameters. In fact, the scanning parameters used for LO_2 samples have a minimum influence on transformation behavior of the SLM parts, especially after solution treatment (Fig. 3b).

The relation between martensite start temperature (M_s) and scanning velocity is shown in Fig. 4. A clear decrease in M_s is observed as scanning velocity increases for samples produced in a HO_2 environment. As seen, the main changes in transformation temperatures with scanning velocity occur for HO_2 samples (over a 65 °C shift across the used scanning parameters). These changes remain almost as it was after solution treatment. In contrast, LO_2 samples demonstrate a small change in transformation temperature before solution treatment (around 20 °C shift across the used scanning parameters) and almost no change after solution treatment.

Composition Analysis

The ICP results comparing as-received powder in comparison to the highest and lowest laser power parameters used are summarized in Table 2. It can be seen that nickel evaporation has occurred for both sets of scanning parameters with the effects seen being more severe at a higher laser power.

Phase Identification

The XRD patterns of as-built samples produced in a low-oxygen atmosphere with different scanning parameters are shown in Fig. 5. It can be seen that secondary phase peaks are at higher intensities at lower laser power and scan speed parameters.

Discussion

This paper investigates the effect of the SLM-processing parameters on the martensitic transformation behavior of NiTi. Primarily, it has been previously shown that for conventionally manufactured binary NiTi, the martensitic transformation temperature is known to decrease with Ni content in a specific Ni range (∼over 50.5 at.%) [9]. In such compositional ranges, the nickel alloy content is the most determinant factor for the transformation criteria.

The changes of Ni composition (due to Ni laser evaporation) are also observed in this work (according to the ICP results shown in Table 2). However, according to the primary powder composition of SLM parts, Ni evaporation is not in the specific range which could strongly increase the DSC transformation temperatures [9] (Figs. 2, 3). In fact, although the SLM parts in this work possessed about 50.0–50.4 at.% Ni, the Ni evaporation could become the main influential factor if the parts contained Ni above 50.5 at.%. Nevertheless, according to ICP results Ni evaporation occurs after SLM, since laser-material interaction can rapidly heat the powder to well above the melting points. This can be intensified once the heating rate increases via higher laser power adjusted to higher scanning speed, as shown in Table 2. This phenomenon should be carefully considered before selection of the primary powder composition, as nickel evaporation after SLM starts from the initial powder (Table 2).

As seen in the XRD spectra (Fig. 5), austenite is clearly becoming more stable at higher laser scanning speeds. Since Ni evaporation had a minimal influence for the current case (owing to the primary composition), other factors appear to be more influential. For example, reduced precipitation due to higher cooling rates of higher laser scanning speed can decrease the transformation temperatures (Fig. 4). Although these very small precipitates have

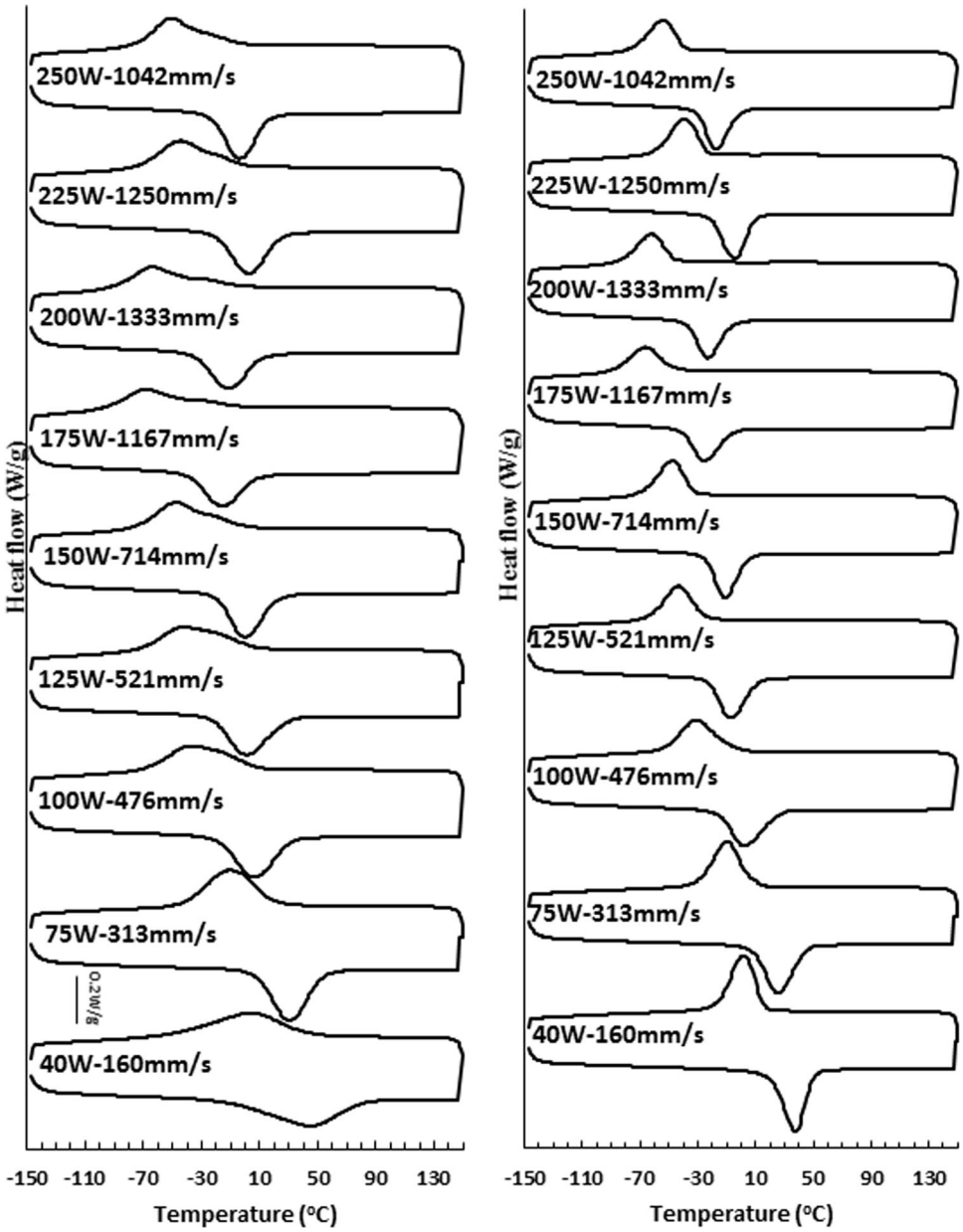

Fig. 2 DSC curves of NiTi samples **a** before and **b** after solution treatment for all SLM parameters used in a relatively high oxygen environment. Additional or broader peaks may appear in some as-SLM curves as an indication for inhomogeneous transformations and/or intermediate phases

a low fraction (that is why they do not appear in XRD spectra, Fig. 5), they should be mainly composed of nickel-rich precipitates such as Ni_4Ti_3. These precipitates may increase the transformation temperatures in Ni-rich NiTi shape-memory alloys by facilitating martensite formation with inducing incoherency stresses, modifying the local Ni-concentrations [18], and acting as martensite nucleation points [17]. In addition to precipitation, higher cooling rates of higher scanning speeds may reduce the grain sizes to a threshold that might perhaps decrease the transformation temperatures (as grains can reach below micron sizes at high SLM velocities [17]). However, this might not be a strong case for the current work as these grain size thresholds are normally reported to be very low (might be less than 100 nm [19, 20]).

According to the above-mentioned effects of precipitation and grain size on transformation temperatures, solution treatment should eliminate the transformation differences by dissolving the precipitates and growing the grains to comparable sizes. Despite this reasonable expectation, solution treatment leads to comparable transformation temperatures only in the case of LO_2 SLM samples, but large transformation differences remain for HO_2 SLM parts (Figs. 2, 3, 4). This illustrates the strong atmospheric influence on the quality of SLM-made NiTi parts. In addition, solution treated parts display narrower peaks

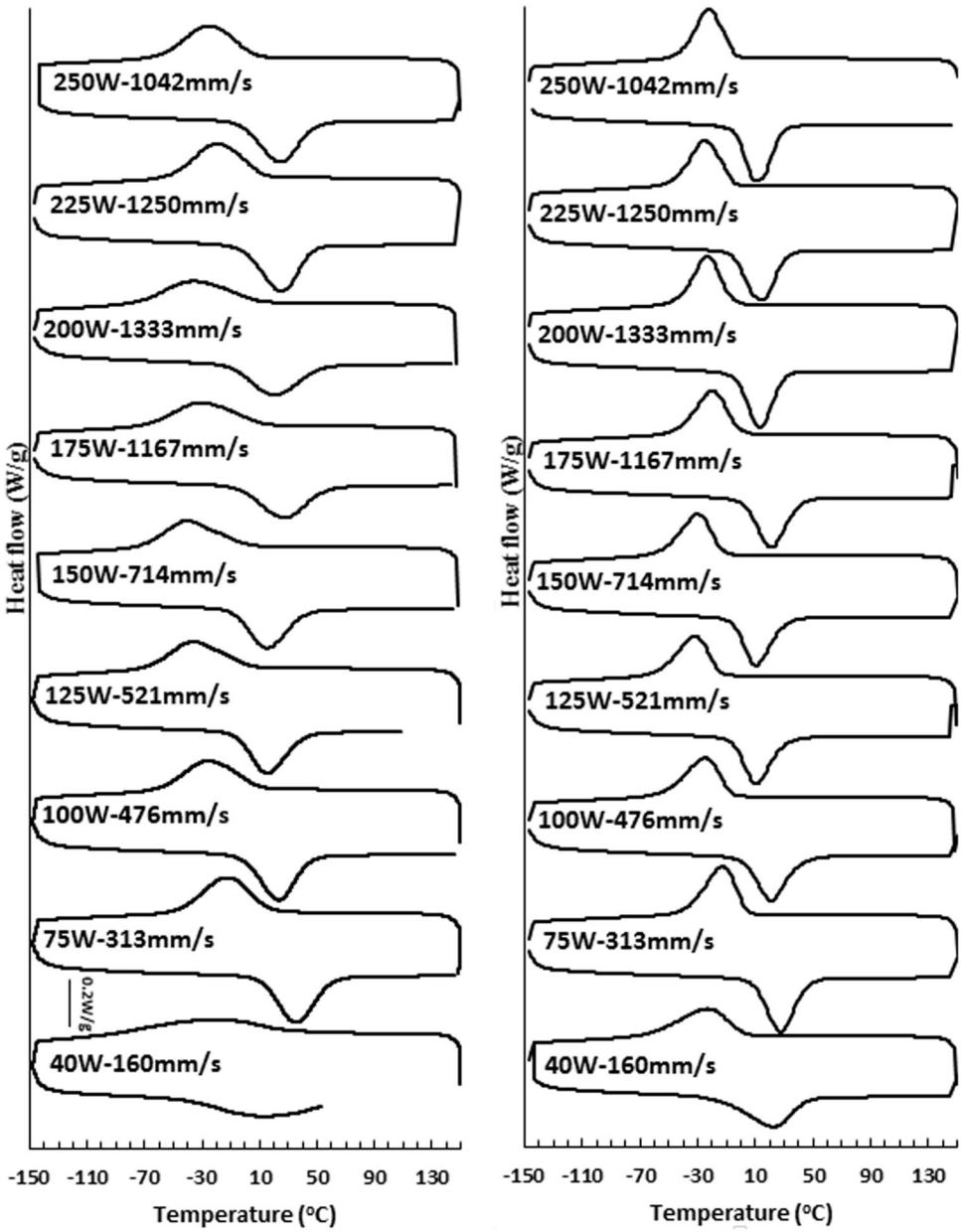

Fig. 3 DSC curves of NiTi samples **a** before and **b** after solution treatment for all SLM parameters used in a low-oxygen environment. Additional or broader peaks may appear in some curves as an indication for inhomogeneous transformations and/or intermediate phases

Table 2 ICP values obtained for NiTi powder as-received and annealed and bulk SLM components

NiTi sample	Processing condition	Ni (wt%)	Ti (wt%)	Ni (at.%)	Ti (at.%)
Original powder	As-received	55.7	44.3	50.6	49.4
	Annealed	55.7	44.3	50.6	49.3
SLM	$P = 40$, $v = 160$, $h = 75$	55.5	44.5	50.4	49.6
	$P = 250$, $v = 1100$, $h = 60$	55.0	44.9	50.0	49.9

P laser power W, v scanning velocity mm s^{-1}, h hatch spacing μm

across all used parameter sets that may improve shape memory quality for potential applications.

In respect of SLM atmospheric influences, oxygen uptake within the alloy during production is clearly controlling the transformation properties of the final component. In a less pure atmosphere, the atmosphere can form oxides or nitrides (such as Ti_4Ni_2O and TiN) [21]. Therefore, higher laser scanning velocity can affect the size/formation of these particles/precipitates and eventually control the transformation temperatures. Similar to other Ni–Ti precipitates, these particles may need to reach an optimum size to facilitate martensitic transformation (e.g.,

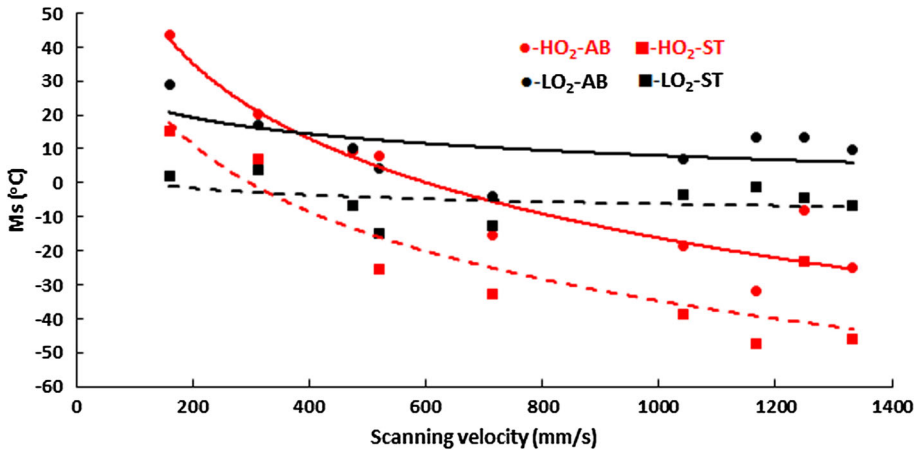

Fig. 4 Variation of M_s temperatures as a function of laser scanning speed for all process conditions

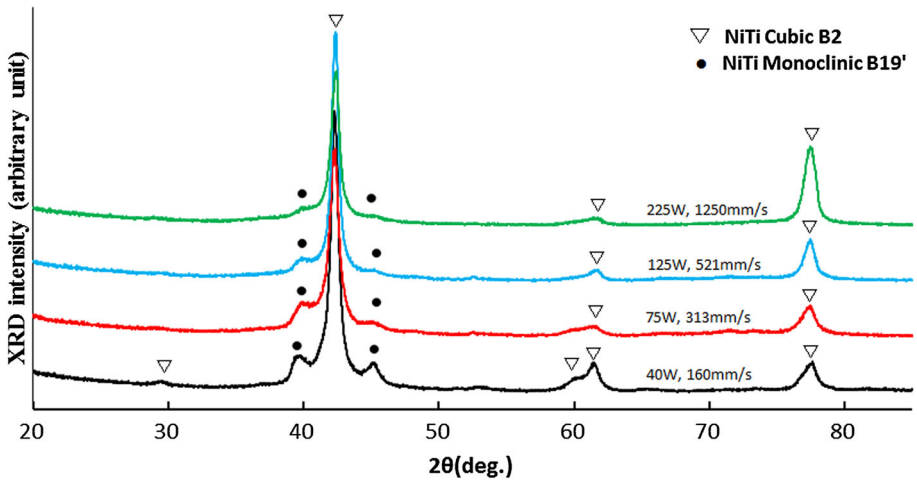

Fig. 5 XRD spectra of the as-built NiTi SLM parts in a low-oxygen environment built with various laser powers

by acting as nucleation sites). Therefore, excessively high laser speeds may completely dissolve the atmospheric impurities within the matrix or lead to extremely fine particles without any influence on martensitic transformation. As these particles do not dissolve in the matrix during the solution treatment, the transformation trend with scanning speed remains unchanged after solution treatment (see Fig. 4).

As appreciated from the above, it is very important to control and monitor the atmospheric impurities (such as oxygen content within the build chamber) besides NiTi compositions during the SLM process. This allows the manipulation of properties using the scanning parameters according to application requirements.

Conclusions

This work aims to further underpin and investigate more deeply the potential factors affecting the transformation temperatures of nitinol parts produced via SLM. Two processing regimes were used in a high- and low-oxygen atmosphere along with a wide range of laser scanning parameters able to produce fully dense parts. It can be confirmed that atmospheric impurities is a highly important issue during SLM and must be controlled accordingly. The findings of this study can be summarized as follows:

(1) It is essential to carefully select the processing parameters during all steps to produce repeatable phase transformation behaviors.
(2) New flushing procedures for the production of nickel titanium via SLM should be created to help minimize impurity (such as oxygen) pick-up during production, as oxidation has been shown to be the dominating factor affecting SLM-produced nickel titanium parts.
(3) M_s is confirmed to decrease with increasing laser scanning speed. Ni evaporation is also confirmed from powder to component which could be an important factor according to the used composition.
(4) Solution treatment can increase the shape-memory quality by sharpening the transformation peaks. Besides, it can undo the influence of dissolvable

Ni–Ti precipitates that might vary according to the used SLM parameters.

Acknowledgments The authors acknowledge support within the EU 7th framework program (FP7) under Marie Curie ITN project Bio-TiNet (Grant No. 264635). Xiebin Wang wishes to thank the Research Foundation Flanders (FWO) under Grant No. G036615N. The assistance from X. Zhang with the XRD measurements and D. Winant with the DSC measurements is highly appreciated.

References

1. Kruth JP, Levy G, Klocke F, Childs THC (2007) Consolidation phenomena in laser and powder-bed based layered manufacturing. CIRP Ann-Manuf Technol 56:730–759
2. Speirs M, Dadbakhsh S, Buls S, Kruth J, Van Humbeeck J, Schrooten J et al (2013) High value manufacturing: advanced research in virtual and rapid prototyping: proceedings of the 6th international conference on advanced research in virtual and rapid prototyping. CRC Press, Boca Raton, pp 309–314
3. Habijan T, Haberland C, Meier H, Frenzel J, Wittsiepe J, Wuwer C et al (2013) The biocompatibility of dense and porous nickel–titanium produced by selective laser melting. Mater Sci Eng C 33:419–426
4. Gotman I, Ben-David D, Unger RE, Böse T, Gutmanas EY, Kirkpatrick CJ (2013) Mesenchymal stem cell proliferation and differentiation on load-bearing trabecular nitinol scaffolds. Acta Biomater 9:8440–8448
5. Elahinia MH, Hashemi M, Tabesh M, Bhaduri SB (2012) Manufacturing and processing of NiTi implants: a review. Prog Mater Sci 57:911–946
6. Van Humbeeck J (1999) Non-medical applications of shape memory alloys. Mater Sci Eng A 273:134–148
7. Duerig T, Pelton A, Stöckel D (1999) An overview of nitinol medical applications. Mater Sci Eng A 273:149–160
8. Frenzel J, Wieczorek A, Opahle I, Maaß B, Drautz R, Eggeler G (2015) On the effect of alloy composition on martensite start temperatures and latent heats in Ni–Ti-based shape memory alloys. Acta Mater 90:213–231
9. Khalil-Allafi J, Amin-Ahmadi B (2009) The effect of chemical composition on enthalpy and entropy changes of martensitic transformations in binary NiTi shape memory alloys. J Alloy Compd 487:363–366
10. Ahadi A, Sun Q (2015) Stress-induced nanoscale phase transition in superelastic NiTi by in situ X-ray diffraction. Acta Mater 90:272–281
11. Frenzel J, Zhang Z, Somsen C, Neuking K, Eggeler G (2007) Influence of carbon on martensitic phase transformations in NiTi shape memory alloys. Acta Mater 55:1331–1341
12. Schetky LM, Wu M (2003) Medical device materials: Proceedings from the materials & processes for medical devices conference 2003. ASM International, Anaheim, pp 271–276
13. Christoph H, Mohammad E, Jason MW, Horst M, Jan F (2014) On the development of high quality NiTi shape memory and pseudoelastic parts by additive manufacturing. Smart Mater Struct 23:104002. doi:10.1088/0964-1726/23/10/104002
14. Dadbakhsh S, Vrancken B, Kruth JP, Luyten J, Van Humbeeck J (2016) Texture and anisotropy in selective laser melting of NiTi alloy. Mater Sci Eng A 650:225–232
15. Brückner F, Lepski D, Beyer E (2007) Modeling the influence of process parameters and additional heat sources on residual stresses in laser cladding. J Therm Spray Technol 16:355–373
16. Bormann T, Schumacher R, Müller B, Mertmann M, de Wild M (2012) Tailoring selective laser melting process parameters for NiTi implants. J Mater Eng Perform 21:2519–2524
17. Dadbakhsh S, Speirs M, Kruth J-P, Schrooten J, Luyten J, Van Humbeeck J (2014) Effect of SLM parameters on transformation temperatures of shape memory nickel titanium parts. Adv Eng Mater 16:1140–1146
18. Schryvers D, Tirry W, Yang Z (2006) Measuring strain fields and concentration gradients around Ni_4Ti_3 precipitates. Mater Sci Eng A 438:485–488
19. Waitz T, Antretter T, Fischer FD, Simha NK, Karnthaler HP (2007) Size effects on the martensitic phase transformation of NiTi nanograins. J Mech Phys Solid 55:419–444
20. Ahadi A, Sun Q (2014) Effects of grain size on the rate-dependent thermomechanical responses of nanostructured superelastic NiTi. Acta Mater 76:186–197
21. Olier P, Barcelo F, Bechade J, Brachet J, Lefevre E, Guenin G (1997) Effects of impurities content (oxygen, carbon, nitrogen) on microstructure and phase transformation temperatures of near equiatomic TiNi shape memory alloys. J Phys 7:C5-143–C5-148